HAL
open science

Universal $G' \sim \mathrm{L}^{--3}$ law for the low-frequency shear modulus of confined liquids

Alessio Zaccone, Laurence Noirez

▶ **To cite this version:**

Alessio Zaccone, Laurence Noirez. Universal $G' \sim \mathrm{L}^{--3}$ law for the low-frequency shear modulus of confined liquids. Journal of Physical Chemistry Letters, 2021, 12, pp.650-657. 10.1021/acs.jpclett.0c02953 . hal-03105598v2

HAL Id: hal-03105598

https://hal.science/hal-03105598v2

Submitted on 4 Nov 2021

HAL is a multi-disciplinary open access archive for the deposit and dissemination of scientific research documents, whether they are published or not. The documents may come from teaching and research institutions in France or abroad, or from public or private research centers.

L'archive ouverte pluridisciplinaire **HAL**, est destinée au dépôt et à la diffusion de documents scientifiques de niveau recherche, publiés ou non, émanant des établissements d'enseignement et de recherche français ou étrangers, des laboratoires publics ou privés.

THE JOURNAL OF PHYSICAL CHEMISTRY LETTERS
A JOURNAL OF THE AMERICAN CHEMICAL SOCIETY

pubs.acs.org/JPCL Perspective

Universal $G' \sim L^{-3}$ Law for the Low-Frequency Shear Modulus of Confined Liquids

Alessio Zaccone* and Laurence Noirez*

Cite This: https://dx.doi.org/10.1021/acs.jpclett.0c02953 Read Online

ACCESS | Metrics & More | Article Recommendations

ABSTRACT: Liquids confined to sub-millimeter scales have remained poorly understood. One of the most striking effects is the large elasticity revealed using good wetting conditions, which grows upon further decreasing the confinement length, L. These systems display a low-frequency shear modulus in the order of 1−10^3 Pa, contrary to our everyday experience of liquids as bodies with a zero low-frequency shear modulus. While early experimental evidence of this effect was met with skepticism and abandoned, further experimental results and, most recently, a new atomistic theoretical framework have confirmed that liquids indeed possess a finite low-frequency shear modulus G', which scales with the inverse cubic power of confinement length L. We show that this law is universal and valid for a wide range of materials (liquid water, glycerol, ionic liquids, non-entangled polymer liquids, isotropic liquids crystals). Open questions and potential applications in microfluidics mechanochemistry, energy, and other fields are highlighted.

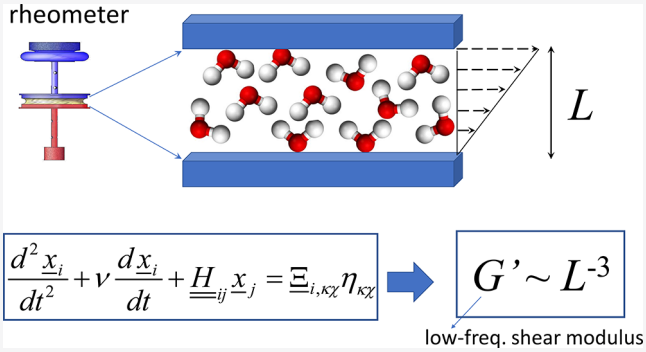

Our daily life experience and education tell us that when a liquid, e.g., liquid water, is subjected to an infinitesimal shear stress, it flows. In physics, the absence of noticeable mechanical resistance can be expressed by saying that the shear elastic modulus G of liquids is exactly zero, where the shear modulus represents the proportionality coefficient between the applied shear stress (σ) and the resulting deformation of a solid body (γ), i.e., Hooke's law, $\sigma = G\gamma$. Here, a first important distinction comes into play, as the above statement is true for nearly static measurements, i.e., at low frequency or low deformation rate, where the shear modulus is zero, but at high frequency or high rate of deformation the shear modulus of liquids is large (as one would experience by diving into a swimming pool from a considerable height, a possibly painful experience if one is not an experienced diver!). This observation reflects the fact that liquids at high frequency of external drive behave like amorphous solids (e.g., glasses), because the atoms or molecules are made to oscillate at such high speed by the external field that they cannot escape the liquid cage made by their nearest neighbors. This goes along with the ability of liquids to sustain transverse acoustic waves at sufficiently high momenta or high frequencies, as predicted in early work by Yakov Frenkel in the 1940s.[1]

Besides this basic notion, which defines the essential property of a liquid, our understanding of the physics of liquids is incomplete.[2] This is due to the fact that atoms and molecules in a liquid are in a state of disorder and random motions, which is very different from atoms or molecules sitting on a regular lattice in crystalline solids. Therefore, it is difficult to find a mathematical description of the atomic or the molecular dynamics in a liquid, from which quantitative explanations of the macroscopic properties of liquids could be deduced.

As a consequence of this state of affairs, it has been impossible so far to rationalize the mechanics of liquids on microscopic scales. Already in 1989−1990, using the newly developed piezo-quartz resonance device, it was experimentally observed that a liquid film confined at a several micrometers scale exhibits an unexpected shear elasticity at low frequency/rate of deformation, a behavior much more akin to solids than to liquids.[3,4] In spite of the fact that these experiments were led by Boris Derjaguin, one of the most prominent Russian physico-chemists of the 20th century, the observation was met with skepticism and abandoned by the scientific community because of the preconceived notion that liquids must have a zero shear modulus. From the early 2000s, many other experiments conducted by different teams across different length scales, however, resulted in the same observation, extending the identification of the "Derjaguin" shear elasticity up to the

Received: September 27, 2020
Accepted: December 23, 2020

© XXXX American Chemical Society

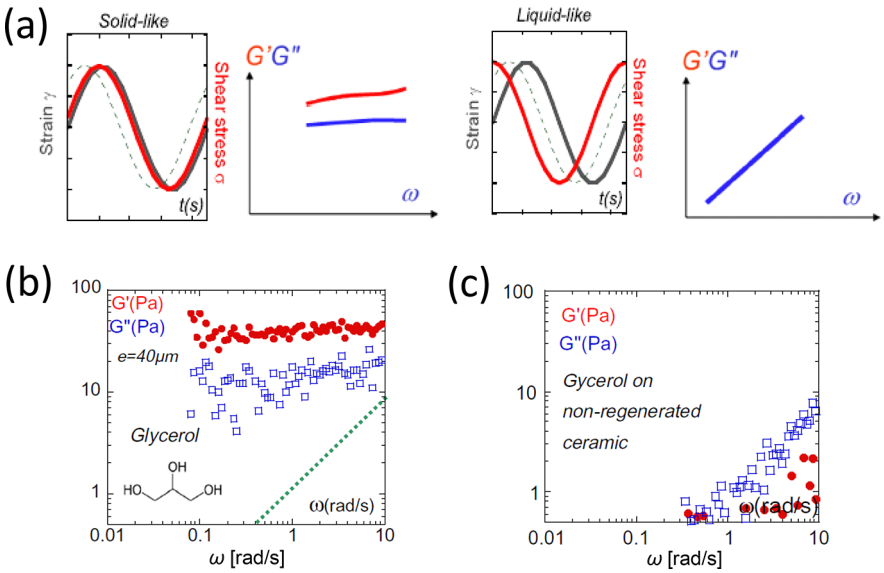

Figure 1. Dynamic viscoelastic response of liquids. Panel (a) shows a schematic depiction of time-dependent shear stress σ and shear strain γ for solid-like (left) and liquid-like (right) systems and the corresponding frequency-dependent viscoelastic curves. The lower set of figures shows the experimentally measured G' and G'' as a function of oscillation frequency ω for glycerol in good (cleaned/thermally regenerated ceramic), panel (b), and poor (non-cleaned ceramic), panel (c), surface-wetting conditions. The measurements are carried out at low gap thickness (e = 0.04 mm) and at room temperature. Panel (b), obtained using a surface state perfectly free of impurities, displays higher viscoelastic moduli and leads to $G' > G''$, indicating a solid-like response. In panel (c), where the thermal regeneration of the surfaces has not been applied (hence causing a lower energy of adhesion, thus poor wetting and possibly de-wetting), G'' scales exactly linear with ω, in line with expectations for purely viscous liquids. Reproduced with permission from ref 19. Copyright 2010 Elsevier.

millimeter scale,[5] using different experimental techniques and different liquids (from liquid water to liquid crystals to ionic liquids and polymer melts).[6−12] A theoretical explanation for these phenomena, however, has remained elusive (despite the keen interest in this problem by Nobel laureate Pierre-Gilles de Gennes, a former colleague of one of us, before his untimely death in 2007).

In Figure 1 is shown the typical viscoelastic response of a sub-millimeter confined liquid (glycerol at room temperature), in terms of the storage shear modulus $G'(\omega)$ and the dissipative loss modulus $G''(\omega)$, which represent, respectively, the real and imaginary parts of the complex shear modulus, $G^* = G'(\omega) + iG''(\omega)$. Here, ω is the frequency of the externally applied mechanical oscillation field (oscillatory strain), $\gamma = \gamma_0 \sin(\omega t)$. The shear strain γ is now time-dependent and triggers, under conditions of the linear response, a stress response, $\sigma = \sigma_0 \sin(\omega t + \delta)$, where δ is a phase which is $\delta = 0$ for a perfectly elastic response (Hooke's law) and $\delta = \pi/2$ for a perfectly fluid response. The situation is summarized in Figure 1a. Experimentally, the solid-like response displays $G' > G''$, and a flat plateau of G' at low frequency. The hallmark of a liquid-like viscous response, instead, is that $G' \ll G'' = \eta\omega$ (where η is the shear viscosity) at low frequency. While bulk liquids have $\delta = \pi/2$ (perfectly viscous response) for low frequencies of oscillation (in the range 0.001−10 Hz), liquids in confined geometry and/or strongly in interaction with the substrate (wetting conditions) may display δ values much smaller than $\pi/2$, which indicates a solid-like viscoelastic response. This goes along with a substantial low-frequency plateau value of storage modulus, $G' > G''$. An experimental example which illustrates the solid-like response of confined liquids is provided in Figure 1b,c, showing the mechanical response of a small-molecule liquid, glycerol, at low frequency and room temperature. Among other simple liquids, very similar mechanical responses at low frequency have been measured for water,[6] for o-terphenyl (OTP),[7] and for ionic liquids.[8] Similar solid-like properties have also been observed with higher-molecular-weight liquids, such as linear alkanes,[9] isotropic liquids crystals,[10] side-chain liquid crystals,[11,12] entangled[7] and non-entangled polymers,[10,13] and supercooled polypropylene glycol.[14] The same phenomena have also been observed at the nanoscale in nano-confined liquids.[15−18]

It is important to note the role of boundary conditions, i.e., of the surface energy. For certain solid surfaces in direct contact with the liquid, the liquid molecules are firmly anchored to the solid surface. This is typically associated with high wettability, or good wetting, of the surface, and implies strong attractive interactions between the liquid molecules and the surface. In order to implement these conditions, therefore, it is also necessary to consider the surface energy of the solid, in addition to cleaned, atomically smooth conditions. If that is not the case, e.g., for non-wetting surfaces, the liquid molecules in direct contact with the surface are instead more free in their relative motion with respect to the solid surface. This makes a big difference in order to access the elastic response. It turns out that, in the case of wetting surfaces, the mechanical response of the confined liquid is higher and solid-like, whereas for non-wetting surfaces, the standard purely viscous response is observed. This phenomenon can be mechanistically explained in terms of plane-wave null boundary conditions for the wetting surfaces (or absence thereof, for non-wetting surfaces) in the following theoretical analysis.

These experimental findings have recently been rationalized from the point of view of theory. Theories of liquids have normally focused on the high-frequency shear modulus for which atomistic or molecular-level expressions are available, such as the Zwanzig−Mountain formula,[20] precisely because the low-frequency mechanical of bulk liquids was not supposed to exist. In the allied field of amorphous solids, such as glasses,

https://dx.doi.org/10.1021/acs.jpclett.0c02953
J. Phys. Chem. Lett. XXXX, XXX, XXX−XXX

instead, the mechanical response has been studied across the entire frequency range, since amorphous solids obviously exhibit a finite zero-frequency shear modulus. In particular, lattice dynamics can be extended to deal with disordered systems where the positions of atoms/molecules are completely random, to arrive at theoretical expressions for the elastic constants and for the viscoleastic moduli.[21] The resulting theoretical framework is sometimes referred to as non-affine lattice dynamics, or NALD.[22,23] The theory has proved effective in quantitatively describing elastic, viscoelastic, and plastic responses of systems as diverse as jammed random packings and random networks,[21] glassy polymers,[24−26] metallic glass,[27] and colloidal glasses.[28] Furthermore, NALD intrinsically takes into account long-range correlation phenomena[29,30] that are present also in liquids and give rise to acoustic wave propagation.

The usual starting point is the equation of motion of a microscopic building block, i.e., an atom or a molecule for atomic liquids or molecular liquids, respectively. In the case of polymers, the building block could be identified with a monomer of the polymer chain.[24] Following previous literature,[21,22] we introduce the Hessian matrix of the system $\underline{\underline{H}}_{ij} = -\partial^2\mathcal{U}/\partial\underline{\mathring{q}}_i\partial\underline{\mathring{q}}_j$, where $\mathcal{U}$ is the internal energy, and the affine force field $\underline{\Xi}_{i,\kappa\chi} = \partial\underline{f}_i/\partial\eta_{\kappa\chi}$, where $\eta_{\kappa\chi}$ is the strain tensor. For example, for simple shear deformation the xy entry of tensor $\eta_{\kappa\chi}$ is given by a scalar γ, i.e., the shear strain introduced above, which coincides with the angle of deformation.

Furthermore, $\underline{\mathring{q}}_i$ is the coordinate of atom i in the initial undeformed frame (denoted with the ring notation), while $\underline{f}_i = \partial\mathcal{U}/\partial\underline{q}_i$ denotes the force acting on atom i in the affine position, i.e., in the initial frame acted upon by the macroscopic deformation, hence the name "affine" force-field. See Figure 2a for a visual representation of affine positions in a deformed frame. Greek indices refer to Cartesian components of the macroscopic deformation (e.g., $\kappa\chi = xy$ for shear). For liquids (and to a lesser extent, also for glasses[24]), the Hessian $\underline{\underline{H}}_{ij}$ is normally evaluated in a reference state obtained from averaging over MD configurations to include instantaneous normal modes, or INMs (purely imaginary vibrational frequencies).[24] For more details about INMs, see ref 31.

As shown in previous works, the equation of motion of atom i in a disordered medium subjected to an external small amplitude strain, in mass-rescaled coordinates, can be written as follows:[22,24]

$$\frac{d^2\underline{x}_i}{dt^2} + \nu\frac{d\underline{x}_i}{dt} + \underline{\underline{H}}_{ij}\underline{x}_j = \underline{\Xi}_{i,\kappa\chi}\eta_{\kappa\chi} \tag{1}$$

where the summation convention is operative for both Latin and Greek indices. Also, $\eta_{\kappa\chi}$ are the components of the Green−Saint Venant strain tensor, and ν is a microscopic friction coefficient which arises from long-range dynamical coupling between atoms mediated by anharmonicity of the pair potential. The term on the right-hand side physically represents the effect of the disordered (non-centrosymmetric) environment leading to non-affine motions: a net force acts on atom i in the affine position (i.e., the position prescribed by the external strain tensor $\eta_{\kappa\chi}$). The situation is schematically depicted in Figure 2b, which contrasts a centrosymmetric environment (left panel), where all atoms are at mechanical equilibrium, even in the affine position (here for an infinitesimal strain), due to cancellation of nearest-neighbor forces that are mirror-images of each other across the central particle, with the situation in a disordered system (liquid or amorphous solid, right panel). In the latter case, the nearest-neighbor forces do not cancel, thus leading to a net force acting on the central atom.

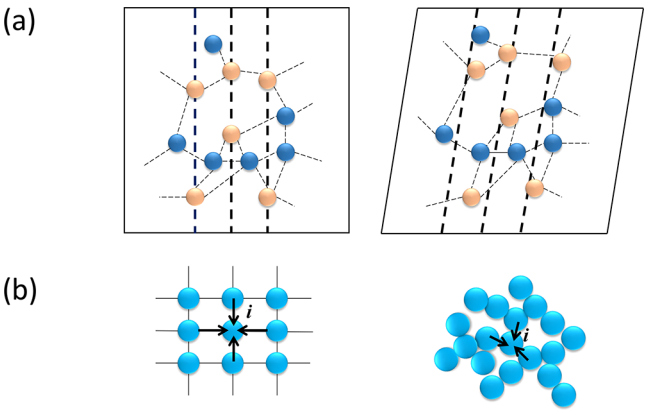

Figure 2. Schematic illustration of non-affine displacements in amorphous media. Panel (a) shows the rearrangements or displacements of atoms upon application of an external shear strain. If the deformation were affine, atoms which sit exactly on the dashed lines in the un-deformed frame (left) would still sit exactly on dashed lines also in the deformed frame (right). However, in a disordered environment this does not happen, and in the deformed frame the atoms that were sitting on the dashed lines in the un-deformed frame are no longer sitting on the dashed lines, but are displaced from them. The distance from the actual positions of the atoms to the dashed line corresponds to the non-affine displacements. Panel (b) provides a visual explanation of the origin of non-affine displacements in disordered environments. The left figure shows a perfect lattice where, upon applying a small deformation, the nearest-neighbor forces from surrounding atoms cancel each other out in the affine positions, so there is no need for non-affine displacements to arise. In the right figure, instead, the tagged atom i is not a center of inversion symmetry, which implies that nearest-neighbor forces from surrounding atoms do not balance in the affine position, and hence a net force arises which triggers the non-affine displacement in order to maintain mechanical equilibrium.

As a consequence, in order to keep mechanical equilibrium on all atoms throughout the deformation, an additional *non-affine* displacement is required in order to relax the force f_i acting in the affine position. This displacement brings each atom i to a new (non-affine) position. A schematic depiction of a non-affine displacement is shown in Figure 2a.

The equation of motion eq 1 can also be derived from first-principles, from a model particle-bath Hamiltonian as shown in previous work.[24] Using standard manipulations (Fourier transformation and eigenmode decomposition from time to eigenfrequency[22]), and applying the definition of mechanical stress, we obtain the following expression for the viscoelastic (complex) elastic constants:[22,24]

$$C_{\alpha\beta\kappa\chi}(\omega) = C^{\text{Born}}_{\alpha\beta\kappa\chi} - \frac{1}{V}\sum_n \frac{\hat{\underline{\Xi}}_{n,\alpha\beta}\hat{\underline{\Xi}}_{n,\kappa\chi}}{\omega^2_{p,n} - \omega^2 + i\omega\nu} \tag{2}$$

where $C^{\text{Born}}_{\alpha\beta\kappa\chi}$ is the Born or affine part of the elastic constant, i.e., what survives in the high-frequency limit. Here, ω represents the oscillation frequency of the external strain field, whereas ω_p denotes the internal eigenfrequency of the liquid (which results, e.g., from diagonalization of the Hessian matrix[24]). We use the notation ω_p to differentiate the eigenfrequency from the external oscillation frequency ω.

https://dx.doi.org/10.1021/acs.jpclett.0c02953
J. Phys. Chem. Lett. XXXX, XXX, XXX−XXX

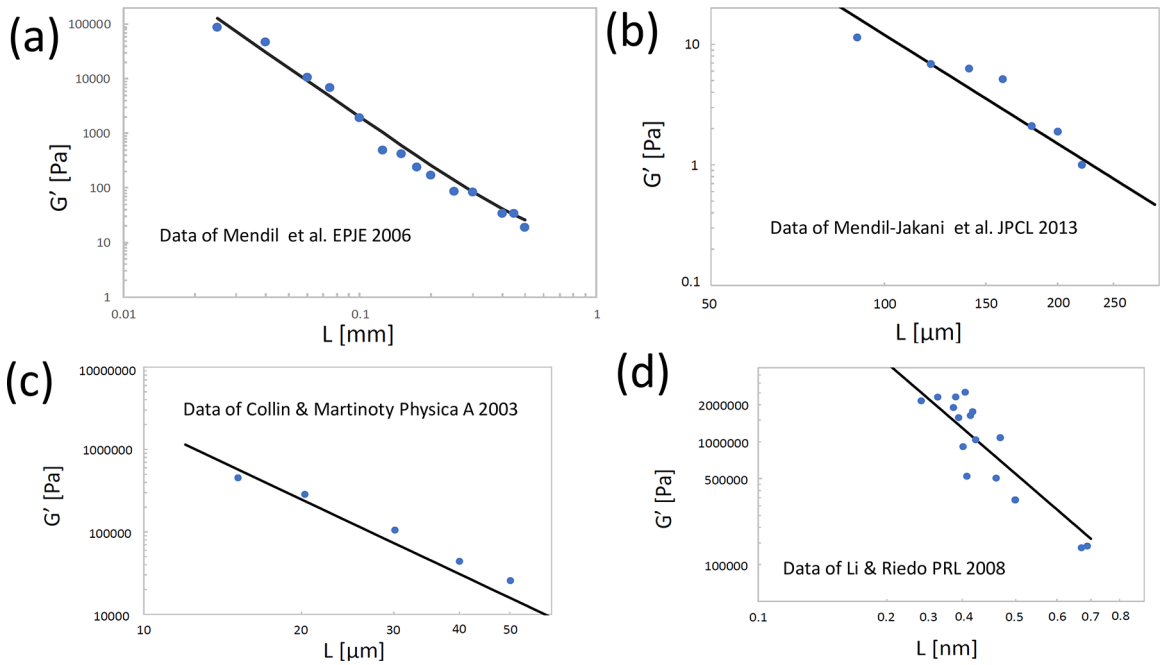

Figure 3. Experimental data of low-frequency shear modulus G' versus confinement length L for different systems, where circles represent experimental data while the solid line is the law $G' \sim L^{-3}$ derived in ref 37. Panel (a) shows the comparison for $PAOCH_3$, an isotropic liquid crystal system from ref 10; (b) shows the same comparison for ionic liquids, from ref 8; (c) shows experimental data for short-chain (non-entangled) polystyrene melts from ref 13; and (d) shows experimental data for nanoconfined water from ref 15.

As already mentioned above, an atomistic expression for $G_\infty \equiv C^{\mathrm{Born}}_{\alpha\beta\kappa\chi}$ is provided by the well-known Zwanzig–Mountain formula,[20] in terms of the pair potential $V(r)$ and the radial distribution function $g(r)$. The sum over n in eq 2 runs over all $3N$ degrees of freedom (given by the atomic or molecular building blocks with central-force interactions). Also, we recognize the typical form of a Green's function, with an imaginary part given by damping and poles $\omega_{p,n}$ that correspond to the eigenfrequencies of the excitations.

At this point we use a key assumption of plane waves; i.e., we assume that, at low values of wavenumber k (i.e., for long wavelengths λ), liquids can support shear elastic waves. Propagation of longitudinal acoustic waves in liquids is, of course, a well-known fact to everyone who does snorkeling or swims under the water level, with firmly established experimental and theoretical evidence of longitudinal acoustic dispersion relations.[32−34] For transverse or shear acoustic waves in liquids, instead, there is no propagation below a characteristic wavenumber. Indeed, there is an onset value of k, that we shall denote k_g, above which these modes can propagate in liquids, known as the k-gap,[2] again a result due originally to Frenkel,[1] and recently demonstrated by Trachenko and co-workers.[35,36]

Following the analytical steps presented in ref 37, we arrive at the following expression for the complex shear modulus:

$$G^*(\omega) = G_\infty - B\int_{1/L}^{k_D} \frac{\omega_{p,L}^2(k)}{\omega_{p,L}^2(k) - \omega^2 + i\omega\nu} k^2\, dk - B\int_{k_{min}}^{k_D} \frac{\omega_{p,T}^2(k)}{\omega_{p,T}^2(k) - \omega^2 + i\omega\nu} k^2\, dk \tag{3}$$

where the first integral represents the non-affine (negative or softening) contribution due to longitudinal (L) acoustic modes, while the second integral represents the non-affine (also softening) contribution due to the transverse (T) acoustic modes. The upper integration limit in the k integrals is set, as usual, by the Debye wavenumber k_D. In the above expression, $k_{min} = \max\left(k_g, \frac{1}{L}\right)$ is an "infrared" cutoff for the transverse modes, with k_g the onset wavenumber for transverse phonons in liquids (the k-gap) and L the confinement length along the z direction. In the above treatment, dealing with plane waves in 3D implies the condition $\sqrt{k_x^2 + k_y^2 + k_z^2} = k = 2\pi/\lambda$, which leads to the spherical integrals of eq 3, with the metric factor k^2.

For the longitudinal modes, one can resort to the Hubbard–Beeby theory of collective longitudinal modes in liquids,[32] which has been shown to provide a good description of experimental data, and thus use eq 43 from ref 32 for $\omega_{p,L}(k)$ inside the integral above. As shown in ref 37, the final result for the low-frequency G' does not depend on the form of the $\omega_{p,L}(k)$ dispersion relation. However, for the mathematical completeness of the theory, it is important to specify which analytical forms for the dispersion relations can be used.

Anyway, upon taking the real part of G^*, which gives the storage modulus G', and focusing on low external oscillation frequencies $\omega \ll \omega_p$ used experimentally, in both integrals the numerator and denominator cancel out, leaving the same expression in both integrals. Therefore, as anticipated above, the final low-frequency result does not depend on the actual form of $\omega_{p,L}(k)$, nor of $\omega_{p,T}(k)$, although the latter, due to the k-gap, plays an important role (see the expression for k_{min} above) in controlling the "infrared" cutoff of the transverse integral. In the experiments where the size effect of confinement is seen, $k_g \ll \frac{1}{L}$,[38] and $k_{min} = \frac{1}{L}$, thus leading to

$$G' = G_\infty - \alpha\int_{1/L}^{k_D} k^2\, dk = G_\infty - \frac{\alpha}{3}k_D^3 + \frac{\beta}{3}L^{-3} \tag{4}$$

For the lower limit of the non-affine integral, we used an "infrared" cutoff,

https://dx.doi.org/10.1021/acs.jpclett.0c02953
J. Phys. Chem. Lett. XXXX, XXX, XXX−XXX

$$k_{\min} \equiv |\mathbf{k}_{\min}| = 2\pi\sqrt{(1/L_x)^2 + (1/L_y)^2 + (1/L)^2} \quad (5)$$

by assuming that the liquid is confined along the z direction, such that $L \equiv L_z \ll L_x, L_y$; the lower limit in the non-affine integral over k-space thus reduces to $1/L$, as displayed in eq 4. A rigorous estimate of the k-integral in eq 4, including exact prefactors, can be found in ref 39.

In eq 4, the only term which depends on the system size is the last term, while α and β are numerical prefactors. In liquids that are in thermodynamic equilibrium and for quasistatic deformations, a different version of the non-affine response formalism called the stress-fluctuation formalism can be used. It has been rigorously demonstrated that the two versions of the formalism are equivalent in ref 40. Using the stress-fluctuation non-affine formalism in combination with standard equilibrium statistical mechanics, it has been shown in ref 41 that the affine or high-frequency (Born) term G_∞ and the negative non-affine term (here, $-\frac{\alpha}{3}k_D^3$) cancel each other out exactly, such that $G'(\omega\to 0) = 0$ for $L\to\infty$ (bulk liquids). Therefore, for liquids under sub-millimeter confinement, only the third term in the above equation survives, and we finally obtain

$$G' \approx \beta' L^{-3} \quad (6)$$

where $\beta' = \beta/3$ is a numerical prefactor. This law was derived for the first time in ref 37. It is worth noticing that G_∞ is independent of L. This fact can be seen, e.g., through the Zwanzig−Mountain formula, where the main contribution to G_∞ is given as an integral that contains $dV(r)/dr$ as a multiplying factor in the integrand, with $dV(r)/dr = 0$ after a few molecular diameters. This, in turn, implies that no dependencies on length scales much larger than the nearest-neighbor cage can be present in G_∞.

The above theory clarifies that the liquid confinement between two plates is able to "remove" certain low-frequency normal-mode collective oscillations of molecules, associated with the non-affine motions (i.e., negative contributions to the elasticity), which are responsible for the fluid response of liquids under standard macroscopic ("unconfined") conditions. These motions are responsible for reducing the shear modulus basically to zero in macroscopic bulk liquids. Under confinement, instead, the shear modulus is non-zero because these collective oscillations modes are suppressed, and the theory of Zaccone and Trachenko[37] provides the universal law by which the shear modulus grows upon reducing the confinement (gap) size. In particular, the static shear modulus grows with the inverse cubic power of the gap size.

In ref 37, the law $G' \sim L^{-3}$ was found to provide a perfect description of experimental data measured in an isotropic liquid crystal system ($PAOCH_3$) upon varying the confinement length using a conventional rheometer. Here, we show that this law appears to be truly universal, and we present theoretical fittings of several, very different systems in Figure 3.

In all these systems, i.e., polymer melts of relatively low molecular weight, isotropic liquid crystals, ionic liquids, and even nano-confined water, the law eq 6 appears robust, as shown in Figure 3. In the case of nano-confined water,[15] one would expect a crossover from $\sim L^{-3}$ into an L^{-1} regime once a 2D monolayer is reached. This is expected because the k-space integral in eq 4 contains a metric factor k in 2D, instead of k^2 for 3D (in fact, k^{d-1} for generic d-dimensional space). This crossover is not seen in the data of Figure 3d, which calls for further investigations, both experimentally and theoretically. Experimental data have also been reported for OTP, an organic liquid (data not shown here).[7] Those data also show the $\sim L^{-3}$ behavior, but the data at the shortest confinement length, ~0.01 mm, suggest the possible existence of a plateau upon going toward lower L, while the experimental accuracy is lowered as the confinement increases. The paucity of experimental data does not allow for drawing a definitive conclusion on this effect (i.e., the possible existence of a plateau in G' at low L in certain systems), which should also be the object of further investigation, both experimentally and in theory.

As mentioned earlier, a crucial role is played by the surface anchoring. The solid-like response of confined liquids is indeed observed mainly for atomically smooth surfaces (crystal planes) or for conditions of good wetting between liquid and solid surfaces (high energy surfaces). Instead, a standard, purely viscous response is reported for non-wetting or poorly wetting surfaces; see Figure 4 for a schematic illustration of two different surface wetting conditions. The same observation has been made in the case of nanoconfined water, with a substantially higher viscosity measured in the case of good wetting in ref 16.

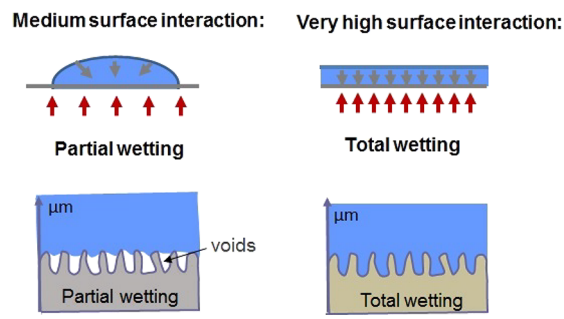

Figure 4. Schematic illustration of different levels of surface interaction between liquid molecules and solid substrate. A not-so-strong attractive interaction leads to partial wetting (left panel), whereas a strong attractive interaction with the solid surface leads to total wetting filling in the rough edges (right panel).

From the theoretical point of view, this fact can be explained by referring to the non-affine lattice dynamic framework summarized above. In particular, wettability connects with the assumption of plane waves and with the implicit *null boundary conditions* for the displacement field of plane waves. This leads straightforward to the term $\sim L^{-3}$ in eq 4 above, which is the term responsible for the solid-like elastic response. Without the full wetting boundary conditions between the liquid and the solid surface, the liquid molecules would not be well-anchored to the solid surface, so the null boundary condition for the acoustic waves would not apply, and the very existence of elastic plane waves would then be called into question. Certainly, the above theoretical framework would not be applicable in that case, as it relies on the ability of the liquid to support plane waves. We can speculate that, when molecules are not anchored to the solid surface, the effective "removal" of softening non-affine motions during the displacement and due to confinement is less effective; hence, the rigidifying effect of "cutting" non-affine motions off due to confinement during the deformation,would not be active. A more precise explanation may require a different theoretical approach, possibly working in eigenfrequency domain rather than in k-space, and is an interesting problem for future research.

Finally, it is important to point out that the non-zero low-frequency shear elasticity has been measured in various liquids irrespective of their surface tension (alkanes, ionic liquids, and

https://dx.doi.org/10.1021/acs.jpclett.0c02953
J. Phys. Chem. Lett. XXXX, XXX, XXX−XXX

polymer melts typically exhibit low surface tension). Since the interfacial (air/liquid) energy scales as the inverse of the surface, significant contributions to G' would be possible if the sample area changes drastically during the oscillatory shear. Bad filling, bad wetting, and large-amplitude oscillator strain (LAOS) conditions could produce a weak "false" torque by breaking the rotational symmetry in the plane.[42] In contrast, the genuine low-frequency shear elasticity intrinsic to the confined liquid state is accessible under conditions where the above artifacts are carefully avoided, and by ensuring a good wetting and low strain—that is, as close as possible to the equilibrium conditions. G' then vanishes by increasing the shear strain (at low gap) to make room for the conventional viscous or viscoplastic flow behavior, which could be understood as the non-linear evolution of the finite low-frequency shear elasticity,[3−7] similar to what happens in amorphous solids upon crossing the yielding/plasticity transition.[27,28]

A number of outstanding questions remain open for future investigations. For example, it could be interesting to explore what kind of connection exists between the above scenario of solid-like elasticity of confined liquids and the glass transition under confinement. The latter is an intensively studied problem, especially in the context of thin polymer films.[43,44] Another important issue is the progress that can be made with numerical simulations. In molecular dynamics (MD), the shear modulus of a confined liquid can be measured, but the noise is currently too large (since the size of MD-simulated systems is small) to make predictions for most realistic situations.[45] Another issue is represented by the small time step used, especially in atomistic simulations (on the order of femtoseconds), which prevents accessing the low-frequency shear modulus. Quasi-static deformation methods implemented atomistically could be a step forward, but they have not demonstrated quantitative predictive power thus far, in comparison with experiments. Also, the power-law nature of the relation $G' \sim L^{-3}$ implies the absence of characteristic length scales (as is typical for power-laws), which suggests that the same mechanisms apply at different length scales; i.e., the same laws apply with L being on the sub-millimeter, micrometer, or nanometer scale. Similarities between trends observed for sub-millimeter[10] and nano-confined fluids,[15,16] in terms of both solid-like mechanical properties and role of wetting,[46] suggest that this may indeed be the case, but further research is required to more firmly establish a complete multi-scale framework.

The potential applications of solid-like elasticity of confined liquids, and its tunability via the control and modulation of the interfacial energy and gap size L, are manifold, encompassing fields as diverse as mechanical stress-assisted manipulation of soft and biological matter in microfluidics,[47−49] protective equipment,[50] biomedical flow applications,[51] oil recovery,[52] heat transfer in liquids,[53] and phase transitions under confinement.[54] Recently, it has been demonstrated that the thermal response of confined liquids is very similar to that of solids,[55] which opens up new opportunities for exploiting thermo-elasticity of confined fluids, e.g., for energy conversion.

Finally, another potential exciting application of this effect is in the emerging fields of mechanochemistry[56−59] and mechanobiology:[60] a (confined) liquid with a finite low-frequency shear modulus G' is able to support mechanical stress-transmission much more efficiently and with much lower dissipative losses compared to standard viscous liquids. This fact may open up new avenues for mechanically induced enhancement of chemical reaction kinetics, by combining the force-transmission efficiency typical of elastic solids with all the favorable solvation and solubility properties of liquids.[61−64]

AUTHOR INFORMATION

Corresponding Authors

Alessio Zaccone − *Department of Physics "A. Pontremoli", University of Milan, 20133 Milan, Italy; Department of Chemical Engineering and Biotechnology and Cavendish Laboratory, University of Cambridge, CB30AS Cambridge, U.K.;* orcid.org/0000-0002-6673-7043; Email: alessio.zaccone@unimi.it

Laurence Noirez − *Laboratoire Léon Brillouin (CEA-CNRS), Université Paris-Saclay, CEA-Saclay, 91191 Gif-sur-Yvette, France*; Email: laurence.noirez@cea.fr

Complete contact information is available at: https://pubs.acs.org/10.1021/acs.jpclett.0c02953

Notes

The authors declare no competing financial interest.

Biographies

Alessio Zaccone

Laurence Noirez

ACKNOWLEDGMENTS

A.Z. thanks Kostya Trachenko and Ivan Kriuchevskyi for enlightening discussions. A.Z. acknowledges financial support from the U.S. Army Research Office, grant no. W911NF-19-2-0055. L.N. expresses her gratitude to the late P.-G. de Gennes and wishes to acknowledge F. Volino for discussions about non-extensive viscoelastic properties.

REFERENCES

(1) Frenkel, J. *Kinetic Theory of Liquids*; Oxford University Press, Oxford, 1946.

(2) Trachenko, K.; Brazhkin, V. V. Collective modes and thermodynamics of the liquid state. *Rep. Prog. Phys.* **2016**, *79*, 016502.

(3) Derjaguin, B.; Bazaron, U.; Zandanova, K.; Budaev, O. The complex shear modulus of polymeric and small-molecule liquids. *Polymer* **1989**, *30*, 97−103.

(4) Derjaguin, B. V.; Bazaron, U. B.; Lamazhapova, K. D.; Tsidypov, B. D. Shear elasticity of low-viscosity liquids at low frequencies. *Phys. Rev. A: At., Mol., Opt. Phys.* **1990**, *42*, 2255−2258.

(5) Noirez, L. Origin of shear-induced phase transitions in melts of liquid-crystal polymers. *Phys. Rev. E* **2005**, *72*, 051701.

(6) Noirez, L.; Baroni, P. Identification of a low-frequency elastic behaviour in liquid water. *J. Phys.: Condens. Matter* **2012**, *24*, 372101.

(7) Noirez, L.; Mendil-Jakani, H.; Baroni, P. Identification of finite shear-elasticity in the liquid state of molecular and polymeric glass-formers. *Philos. Mag.* **2011**, *91*, 1977−1986.

(8) Mendil-Jakani, H.; Baroni, P.; Noirez, L.; Chancelier, L.; Gebel, G. Highlighting a Solid-Like Behavior in Tri-octylmethylammonium Bis(trifluoromethanesulfonyl)imide. *J. Phys. Chem. Lett.* **2013**, *4*, 3775−3778.

(9) Noirez, L.; Baroni, P.; Cao, H. Identification of Shear Elasticity at Low Frequency in Liquid n-Heptadecane, Liquid Water and RT-Ionic Liquids [emim][Tf2N]. *J. Mol. Liq.* **2012**, *176*, 71−75 (Special Issue on Dynamics and Phase Transition: Selected Papers on Molecular Liquids presented at the EMLG/JMLG 2011 Annual Meeting 11−15 September 2011).

(10) Mendil, H.; Baroni, P.; Noirez, L. Solid-like rheological response of non-entangled polymers in the molten state. *Eur. Phys. J. E: Soft Matter Biol. Phys.* **2006**, *19*, 77−85.

(11) Gallani, J. L.; Hilliou, L.; Martinoty, P.; Keller, P. Abnormal viscoelastic behavior of side-chain liquid-crystal polymers. *Phys. Rev. Lett.* **1994**, *72*, 2109−2112.
(12) Martinoty, P.; Hilliou, L.; Mauzac, M.; Benguigui, L.; Collin, D. Side-Chain Liquid-Crystal Polymers: Gel-like Behavior below Their Gelation Points. *Macromolecules* **1999**, *32*, 1746−1752.
(13) Collin, D.; Martinoty, P. Dynamic macroscopic heterogeneities in a flexible linear polymer melt. *Phys. A* **2003**, *320*, 235−248.
(14) Chushkin, Y.; Caronna, C.; Madsen, A. Low-frequency elastic behavior of a supercooled liquid. *EPL (Europhysics Letters)* **2008**, *83*, 36001.
(15) Li, T.-D.; Riedo, E. Nonlinear Viscoelastic Dynamics of Nanoconfined Wetting Liquids. *Phys. Rev. Lett.* **2008**, *100*, 106102.
(16) Ortiz-Young, D.; Chiu, H.-C.; Kim, S.; Voïtchovsky, K.; Riedo, E. The interplay between apparent viscosity and wettability in nano-confined water. *Nat. Commun.* **2013**, *4*, 2482.
(17) Monet, G.; Paineau, E.; Chai, Z.; Amara, M. S.; Orecchini, A.; Jimenéz-Ruiz, M.; Ruiz-Caridad, A.; Fine, L.; Rouzière, S.; Liu, L.-M.; Teobaldi, G.; Rols, S.; Launois, P. Solid wetting-layers in inorganic nano-reactors: the water in imogolite nanotube case. *Nanoscale Adv.* **2020**, *2*, 1869−1877.
(18) Ito, K.; Faraone, A.; Tyagi, M.; Yamaguchi, T.; Chen, S.-H. Nanoscale dynamics of water confined in ordered mesoporous carbon. *Phys. Chem. Chem. Phys.* **2019**, *21*, 8517−8528.
(19) Noirez, L.; Baroni, P. Revealing the solid-like nature of glycerol at ambient temperature. *J. Mol. Struct.* **2010**, *972*, 16−21 (Horizons in hydrogen bond research 2009).
(20) Zwanzig, R.; Mountain, R. D. High-frequency elastic moduli of simple fluids. *J. Chem. Phys.* **1965**, *43*, 4464−4471.
(21) Zaccone, A.; Scossa-Romano, E. Approximate analytical description of the nonaffine response of amorphous solids. *Phys. Rev. B: Condens. Matter Mater. Phys.* **2011**, *83*, 184205.
(22) Lemaître, A.; Maloney, C. Sum Rules for the Quasi-Static and Visco-Elastic Response of Disordered Solids at Zero Temperature. *J. Stat. Phys.* **2006**, *123*, 415.
(23) Zaccone, A. Elastic Deformations in Covalent Amorphous Solids. *Mod. Phys. Lett. B* **2013**, *27*, 1330002.
(24) Palyulin, V. V.; Ness, C.; Milkus, R.; Elder, R. M.; Sirk, T. W.; Zaccone, A. Parameter-free predictions of the viscoelastic response of glassy polymers from non-affine lattice dynamics. *Soft Matter* **2018**, *14*, 8475−8482.
(25) Ness, C.; Palyulin, V. V.; Milkus, R.; Elder, R.; Sirk, T.; Zaccone, A. Nonmonotonic dependence of polymer-glass mechanical response on chain bending stiffness. *Phys. Rev. E: Stat. Phys., Plasmas, Fluids, Relat. Interdiscip. Top.* **2017**, *96*, 030501.
(26) Elder, R. M.; Zaccone, A.; Sirk, T. W. Identifying Nonaffine Softening Modes in Glassy Polymer Networks: A Pathway to Chemical Design. *ACS Macro Lett.* **2019**, *8*, 1160−1165.
(27) Zaccone, A.; Schall, P.; Terentjev, E. M. Microscopic origin of nonlinear nonaffine deformation in bulk metallic glasses. *Phys. Rev. B: Condens. Matter Mater. Phys.* **2014**, *90*, 140203.
(28) Laurati, M.; Maßhoff, P.; Mutch, K. J.; Egelhaaf, S. U.; Zaccone, A. Long-Lived Neighbors Determine the Rheological Response of Glasses. *Phys. Rev. Lett.* **2017**, *118*, 018002.
(29) Shelton, D. P. Long-range orientation correlation in water. *J. Chem. Phys.* **2014**, *141*, 224506.
(30) Zhang, Z.; Kob, W. Revealing the three-dimensional structure of liquids using four-point correlation functions. *Proc. Natl. Acad. Sci. U. S. A.* **2020**, *117*, 14032−14037.
(31) Stratt, R. M. The Instantaneous Normal Modes of Liquids. *Acc. Chem. Res.* **1995**, *28*, 201−207.
(32) Hubbard, J.; Beeby, J. L. Collective motion in liquids. *J. Phys. C: Solid State Phys.* **1969**, *2*, 556−571.
(33) Takeno, S.; Goda, M. A Theory of Phonon-Like Excitations in Non-Crystalline Solids and Liquids. *Prog. Theor. Phys.* **1972**, *47*, 790−806.
(34) Hansen, J.-P.; McDonald, I. R. *Theory of Simple Liquids*; Elsevier, Amsterdam, 2013.
(35) Yang, C.; Dove, M. T.; Brazhkin, V. V.; Trachenko, K. Emergence and Evolution of the *k* Gap in Spectra of Liquid and Supercritical States. *Phys. Rev. Lett.* **2017**, *118*, 215502.
(36) Khusnutdinoff, R. M.; Cockrell, C.; Dicks, O. A.; Jensen, A. C. S.; Le, M. D.; Wang, L.; Dove, M. T.; Mokshin, A. V.; Brazhkin, V. V.; Trachenko, K. Collective modes and gapped momentum states in liquid Ga: Experiment, theory, and simulation. *Phys. Rev. B: Condens. Matter Mater. Phys.* **2020**, *101*, 214312.
(37) Zaccone, A.; Trachenko, K. Explaining the low-frequency shear elasticity of confined liquids. *Proc. Natl. Acad. Sci. U. S. A.* **2020**, *117*, 19653−19655.
(38) Jackson, J. K.; De Rosa, M. E.; Winter, H. H. Molecular Weight Dependence of Relaxation Time Spectra for the Entanglement and Flow Behavior of Monodisperse Linear Flexible Polymers. *Macromolecules* **1994**, *27*, 2426−2431.
(39) Phillips, A. E.; Baggioli, M.; Sirk, T. W.; Trachenko, K.; Zaccone, A. Universal L^{-3} finite-size effects in the viscoelasticity of confined amorphous systems. *arXiv e-Prints* **2020**, No. arXiv:2012.05149[cond-mat.soft].
(40) Mizuno, H.; Silbert, L. E.; Sperl, M.; Mossa, S.; Barrat, J.-L. Cutoff nonlinearities in the low-temperature vibrations of glasses and crystals. *Phys. Rev. E: Stat. Phys., Plasmas, Fluids, Relat. Interdiscip. Top.* **2016**, *93*, 043314.
(41) Wittmer, J. P.; Xu, H.; Polińska, P.; Weysser, F.; Baschnagel, J. Shear modulus of simulated glass-forming model systems: Effects of boundary condition, temperature, and sampling time. *J. Chem. Phys.* **2013**, *138*, 12A533.
(42) Johnston, M. T.; Ewoldt, R. H. Precision rheometry: Surface tension effects on low-torque measurements in rotational rheometers. *J. Rheol.* **2013**, *57*, 1515−1532.
(43) Napolitano, S.; Glynos, E.; Tito, N. B. Glass transition of polymers in bulk, confined geometries, and near interfaces. *Rep. Prog. Phys.* **2017**, *80*, 036602.
(44) Napolitano, S.; Wübbenhorst, M. The lifetime of the deviations from bulk behaviour in polymers confined at the nanoscale. *Nat. Commun.* **2011**, *2*, 260.
(45) George, G.; Kriuchevskyi, I.; Meyer, H.; Baschnagel, J.; Wittmer, J. P. Shear-stress relaxation in free-standing polymer films. *Phys. Rev. E: Stat. Phys., Plasmas, Fluids, Relat. Interdiscip. Top.* **2018**, *98*, 062502.
(46) Bonn, D.; Eggers, J.; Indekeu, J.; Meunier, J.; Rolley, E. Wetting and spreading. *Rev. Mod. Phys.* **2009**, *81*, 739−805.
(47) Graziano, R.; Preziosi, V.; Uva, D.; Tomaiuolo, G.; Mohebbi, B.; Claussen, J.; Guido, S. The microstructure of Carbopol in water under static and flow conditions and its effect on the yield stress. *J. Colloid Interface Sci.* **2021**, *582*, 1067−1074.
(48) Conchúir, B. O.; Zaccone, A. Mechanism of flow-induced biomolecular and colloidal aggregate breakup. *Phys. Rev. E* **2013**, *87*, 032310.
(49) Matthews, H. K.; Ganguli, S.; Plak, K.; Taubenberger, A. V.; Win, Z.; Williamson, M.; Piel, M.; Guck, J.; Baum, B. Oncogenic Signaling Alters Cell Shape and Mechanics to Facilitate Cell Division under Confinement. *Dev. Cell* **2020**, *52*, 563−573.
(50) Elder, R. M.; Knorr, D. B.; Andzelm, J. W.; Lenhart, J. L.; Sirk, T. W. Nanovoid formation and mechanics: a comparison of poly-(dicyclopentadiene) and epoxy networks from molecular dynamics simulations. *Soft Matter* **2016**, *12*, 4418−4434.
(51) Miccio, L.; Cimmino, F.; Kurelac, I.; Villone, M. M.; Bianco, V.; Memmolo, P.; Merola, F.; Mugnano, M.; Capasso, M.; Iolascon, A.; Maffettone, P. L.; Ferraro, P. Perspectives on liquid biopsy for label-free detection of "circulating tumor cells" through intelligent lab-on-chips. *View* **2020**, *1*, 20200034.
(52) Lv, P.; Yang, Z.; Hua, Z.; Li, M.; Lin, M.; Dong, Z. Measurement of viscosity of liquid in micro-crevice. *Flow Meas. Instrum.* **2015**, *46*, 72−79.
(53) Cheng, B.; Frenkel, D. Computing the Heat Conductivity of Fluids from Density Fluctuations. *Phys. Rev. Lett.* **2020**, *125*, 130602.
(54) Jung, G.; Petersen, C. F. Confinement-induced demixing and crystallization. *Phys. Rev. Research* **2020**, *2*, 033207.

https://dx.doi.org/10.1021/acs.jpclett.0c02953
J. Phys. Chem. Lett. XXXX, XXX, XXX−XXX

(55) Kume, E.; Baroni, P.; Noirez, L. Strain-induced violation of temperature uniformity in mesoscale liquids. *Sci. Rep.* **2020**, *10*, 13340.
(56) Do, J.-L.; Friščić, T. Mechanochemistry: A Force of Synthesis. *ACS Cent. Sci.* **2017**, *3*, 13−19.
(57) Howard, J. L.; Cao, Q.; Browne, D. L. Mechanochemistry as an emerging tool for molecular synthesis: what can it offer? *Chem. Sci.* **2018**, *9*, 3080−3094.
(58) van Galen, M.; van der Gucht, J.; Sprakel, J. Chemical Design Model for Emergent Synthetic Catch Bonds. *Front. Phys.* **2020**, *8*, 361.
(59) Klein, I. M.; Husic, C. C.; Kovács, D. P.; Choquette, N. J.; Robb, M. J. Validation of the CoGEF Method as a Predictive Tool for Polymer Mechanochemistry. *J. Am. Chem. Soc.* **2020**, *142*, 16364−16381.
(60) Michels, L.; Gorelova, V.; Harnvanichvech, Y.; Borst, J. W.; Albada, B.; Weijers, D.; Sprakel, J. Complete microviscosity maps of living plant cells and tissues with a toolbox of targeting mechanoprobes. *Proc. Natl. Acad. Sci. U. S. A.* **2020**, *117*, 18110−18118.
(61) Hickenboth, C. R.; Moore, J. S.; White, S. R.; Sottos, N. R.; Baudry, J.; Wilson, S. R. Biasing reaction pathways with mechanical force. *Nature* **2007**, *446*, 423−427.
(62) Konda, S. S. M.; Brantley, J. N.; Bielawski, C. W.; Makarov, D. E. Chemical reactions modulated by mechanical stress: Extended Bell theory. *J. Chem. Phys.* **2011**, *135*, 164103.
(63) Konda, S. S. M.; Avdoshenko, S. M.; Makarov, D. E. Exploring the topography of the stress-modified energy landscapes of mechanosensitive molecules. *J. Chem. Phys.* **2014**, *140*, 104114.
(64) Roessler, A. G.; Zimmerman, P. M. Examining the Ways To Bend and Break Reaction Pathways Using Mechanochemistry. *J. Phys. Chem. C* **2018**, *122*, 6996−7004.

https://dx.doi.org/10.1021/acs.jpclett.0c02953
J. Phys. Chem. Lett. XXXX, XXX, XXX−XXX